Applied Mathematical Modelling 151 (2026) 116488

Contents lists available at ScienceDirect

Applied Mathematical Modelling

journal homepage: www.elsevier.com/locate/apm

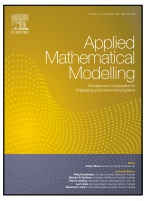

Third moment method for reliability analysis involving independent parametric probability-boxes

Bo-Yu Wang [a], Xuan-Yi Zhang [a,b,*], Yan-Gang Zhao [a], Marcos A. Valdebenito [b], Matthias G.R. Faes [b,c]

[a] National Key Laboratory of Bridge Safety and Resilience, Beijing University of Technology, Beijing, 100124, China
[b] Chair for Reliability Engineering, TU Dortmund University, Leonhard-Euler-Str. 5, Dortmund, 44227, Germany
[c] International Joint Research Center for Engineering Reliability and Stochastic Mechanics, Tongji University, Shanghai, 200092, China

ARTICLE INFO

Keywords:
Structural reliability analysis
Hybrid uncertainty
Parametric probability boxes
First three moments
Nonlinear performance function

ABSTRACT

Reliability analysis aims to evaluate the failure probability of a structure or structural system under the presence of aleatory uncertainties. However, in practical cases, aleatory uncertainties may be accompanied by uncertainties of the epistemic type, leading to a so-called hybrid problem. These hybrid uncertainties can be modeled in certain cases using probability distributions with parameters characterized as intervals, leading to so-called parametric probability-boxes. In this study, a third moment method is proposed for reliability analysis involving independent parametric probability-boxes. Uncertainties in the first three moments of random variables are considered and modeled by intervals. With the aid of third moment normal transformation techniques, the values of uncertain moments of each parametric probability-box that lead to the bounds of failure probability are determined. Then, the bounds of failure probability can be evaluated by performing two reliability analyses. The application of the proposed method is illustrated by both numerical and practical examples, including nonlinear and finite element problems.

1. Introduction

The reliability of a structure or structural system is significantly affected by uncertainties, which are broadly categorized as aleatory (inherent randomness) and epistemic (lack of knowledge). In practical applications, these two types of uncertainty often coexist, and a key challenge is to perform reliability analysis with limited data and imperfect models [1]. Parametric probability boxes (p-boxes) [2–4] have emerged as an effective tool for this purpose, modeling aleatory uncertainty through probability distributions whose parameters are uncertain and described by intervals to capture epistemic uncertainty.

The primary goal when using parametric p-boxes is to determine the bounds of the failure probability. Current approaches can be broadly grouped into two categories. One approach to find the bounds of the failure probability considering parametric p-boxes is the interval Monte Carlo Simulation (IMCS) [5], which applies interval analysis for different realizations of the aleatory variables. Although IMCS is theoretically straightforward, it relies on a large amount of samples to ensure its effectiveness and robustness, posing numerical challenges, especially for problems with small failure probability. To overcome this issue, advanced sample-based methods have been developed to increase the calculation efficiency, such as importance sampling [6,7], directional importance sampling [8,9], extended Monte Carlo simulation [10] and multilevel quasi-Monte Carlo method [11]. However, these sample-based methodologies

* Corresponding author.
E-mail address: zhangxuanyi@bjut.edu.cn (X.-Y. Zhang).

https://doi.org/10.1016/j.apm.2025.116488
Received 30 May 2025; Received in revised form 29 September 2025; Accepted 3 October 2025
Available online 8 October 2025

heavily depend on the quality of generated samples and inevitably suffer from computational inefficiency when dealing with problems involving small failure probabilities.

Another approach for estimating failure probability considering parametric p-boxes is analytical methods. Theoretical solutions can only be achieved for specific cases, i.e., performance function defined by a summation of independent normal random variables and multiplication of independent lognormal random variables [12]. As an alternative, reliability analysis considering parametric p-boxes is defined as a double-loop optimization problem [13]. Since the optimization has to be carried out over the set of all possible combinations of distribution parameters, it is potentially very complicated and computationally expensive. A variety of decoupling methods have been proposed to streamline the optimization process, which aim to separate the propagation of aleatory and epistemic uncertainties and thereby breaking the double-loop, such as a single-loop method based on monotonicity analysis [14] or linear programming-based method [15]. Nevertheless, these methodologies still rely on optimization and may encounter inefficiency with high-dimensional uncertain parameters. To address this issue, the operator norm framework [16,17] was proposed, replacing the double-loop with two deterministic optimizations and two crisp reliability estimations. Although the operator norm framework offers significant advantages in practical applications, it is limited when dealing with strongly nonlinear problems. The class of surrogate methods aims to approximate the performance function by computationally efficient surrogate models, which leads to the increase of computational efficiency of reliability analysis.

In addition to the generally applicable methods, some specific methods can directly determine the values of uncertain parameters that lead to the bounds of failure probability, eliminating the optimization and significantly reducing computational cost. For instance, a third-moment method has been proposed for cases where the performance function is monotonic with respect to random variables characterized by parametric p-boxes (TMI) [18]. This method uses third-moment normal transformation techniques to determine the uncertain moments of parametric p-boxes for the bounds of failure probability. However, a limitation remains in the assumption that there is a single uncertain distribution parameter for each parametric p-box, which may not always hold true in real-world scenarios.

Building upon the foundation established by TMI method [18], this paper proposes a new third moment method involving independent parametric p-boxes, hereinafter referred to as TIPP. The primary contributions of this work are:

(1) The proposed TIPP method overcomes a primary limitation of existing approaches by simultaneously accommodating multiple uncertain moments for a single random variable.
(2) A novel and highly efficient computational procedure is established. This procedure allows for the determination of failure probability bounds with only two classical reliability analyses, thereby circumventing computationally expensive nested-loop optimizations or iterative searches.

The remainder of this paper is organized as follows. Section 2 gives the problem statement. Section 3 and Section 4 propose TIPP method, including the detailed theoretical derivation of uncertain moment values at the bounds, as well as summarizing the straightforward procedure. Section 5 presents the exemplary case studies for validation. Finally, Section 6 provides concluding remarks and an outlook for future research.

2. Problem statement

2.1. Failure probability with uncertain moments

The state of a structure is mathematically defined by the sign of its performance function $G(\mathbf{X})$: the safe and failure domains correspond to $G(\mathbf{X}) > 0$ and $G(\mathbf{X}) < 0$, respectively. The condition $G(\mathbf{X}) = 0$ defines the limit state. $\mathbf{X} = \left(X_1, \ldots X_i, \ldots X_n\right)^{\mathrm{T}}$ is an n-dimensional vector of independent random variables, where X_i is the i-th random variable.

The failure probability is the probability that a structure fails, and can be calculated by the multifold probability integral of the joint probability density function (JPDF) of $\mathbf{X}$ over failure domain. With the consideration of epistemic uncertainty, the JPDF of $\mathbf{X}$ is unknown. In this study, the epistemic uncertainty is addressed by modeling the uncertain moments associated with the JPDF as interval variables. Then, the failure probability can be formulated as a function of uncertain moments $\boldsymbol{\theta}$ as follows:

$$P_f(\boldsymbol{\theta}) = \int_{\Omega_{\mathbf{X}}} I_{\mathbf{X}}(\mathbf{x}) f_{\mathbf{X}}(\mathbf{x}|\boldsymbol{\theta}) d\mathbf{x}, \quad \boldsymbol{\theta} \in \boldsymbol{\Theta}^I . \tag{1}$$

with

$$I_{\mathbf{X}}(\mathbf{X}) = \begin{cases} 1, & G(\mathbf{X}) \le 0 \\ 0, & G(\mathbf{X}) > 0 \end{cases} . \tag{2}$$

where $P_f(\boldsymbol{\theta})$ is the failure probability function; $\Omega_{\mathbf{X}} \in \mathbb{R}^n$ denotes the domain of $\mathbf{X}$; $I_{\mathbf{X}}(\cdot)$ is the indicator function based on $G(\mathbf{X})$; $f_{\mathbf{X}}(\mathbf{X}|\boldsymbol{\theta})$ is the JPDF of $\mathbf{X}$ for a given $\boldsymbol{\theta}$; $\boldsymbol{\theta} \in \boldsymbol{\Theta}^I$ is a realization of uncertain moments of $\mathbf{X}$; and $\boldsymbol{\Theta}^I$ is the support domain of $\boldsymbol{\theta}$, where the bounds of $\boldsymbol{\theta}$ are provided. In this study, the uncertainties in the first three moments of $\mathbf{X}$ are considered.

Based on $P_f(\boldsymbol{\theta})$ given in Eq. (1), the reliability index can be obtained as a function of $\boldsymbol{\theta}$ as follows:

$$\beta(\boldsymbol{\theta}) = -\Phi^{-1}\left[P_f(\boldsymbol{\theta})\right], \quad \boldsymbol{\theta} \in \boldsymbol{\Theta}^I, \tag{3}$$

where $\Phi[\cdot]$ is the cumulative distribution function (CDF) of the standard normal distribution.

With the uncertain moments modeled by interval variables, both $P_f(\boldsymbol{\theta})$ and $\beta(\boldsymbol{\theta})$ are uncertain, while their bounds can be estimated. Thus, instead of computing the exact value of failure probability and reliability index, the aim of this study is to find their bounds, denoted by P_f^I and β^I, respectively.

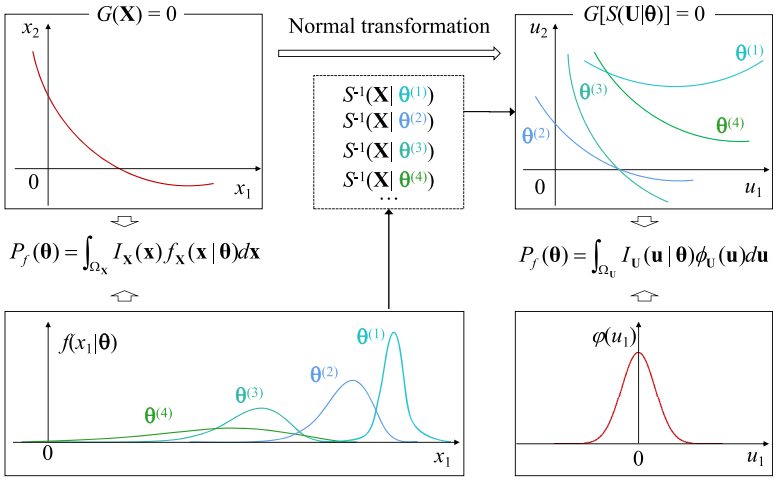

Fig. 1. Schematic graph of uncertainty propagation.

2.2. Bounds of failure probability based on parametric p-boxes

Based on Eq. (1), the uncertainty in θ is propagated through $f_{\mathbf{X}}(\mathbf{X}|\theta)$ to $P_f(\theta)$. As the relationship between $f_{\mathbf{X}}(\mathbf{X}|\theta)$ and $P_f(\theta)$ is difficult to determine explicitly, direct estimation of P_f^I based on Eq. (1) is generally impossible. To facilitate the derivation, $\mathbf{X}$ is mapped into a vector of independent standard normal random variables $\mathbf{U}$ based on the moments, and then $P_f(\theta)$ is redefined in Gaussian space as follows:

$$P_f(\theta) = \int_{\Omega_{\mathbf{U}}} I_{\mathbf{U}}(\mathbf{U}|\theta)\boldsymbol{\phi}_{\mathbf{U}}(\mathbf{u})d\mathbf{u}, \quad \theta \in \boldsymbol{\Theta}^I, \tag{4}$$

where $\Omega_{\mathbf{U}} \in \mathbb{R}^n$ denotes the domain of $\mathbf{U}$; $\boldsymbol{\phi}_{\mathbf{U}}(\mathbf{u}) = \prod_{i=1}^{n} \varphi(u_i)$ is the JPDF of $\mathbf{U}$, which follows a standard Gaussian distribution in n dimensions; and $I_{\mathbf{U}}(\mathbf{U}|\theta)$ is the indicator function defined in Gaussian space, which is defined as follows:

$$I_{\mathbf{U}}(\mathbf{U}|\theta) = I_{\mathbf{X}}[S(\mathbf{U}|\theta)], \quad \theta \in \boldsymbol{\Theta}^I, \tag{5}$$

where $S(\mathbf{U}|\theta)$ is the inverse normal transformation function defined based on the first three moments of $\mathbf{X}$. Based on Eq. (4) and considering that $\boldsymbol{\phi}_{\mathbf{U}}(\mathbf{U})$ is not related with θ, the uncertainty in θ propagates through $S(\mathbf{U}|\theta)$ to the performance function $G[S(\mathbf{U}|\theta)]$ and the indicator function $I_{\mathbf{U}}(\mathbf{U}|\theta)$ in Gaussian space, and then the failure probability $P_f(\theta)$. For illustration, the uncertainty propagation based on Eqs. (1) and (4) are compared in Fig. 1.

Based on Eq. (4), P_f^I can be expressed as [18]:

$$P_f^I = [\underline{P}_f, \overline{P}_f], \tag{6}$$

$$\underline{P}_f = \int_{\Omega_{\mathbf{U}}} I_{\mathbf{U}}(\mathbf{U}|\boldsymbol{\Theta}_{\text{low}})\boldsymbol{\phi}_{\mathbf{U}}(\mathbf{u})d\mathbf{u}, \quad \overline{P}_f = \int_{\Omega_{\mathbf{U}}} I_{\mathbf{U}}(\mathbf{U}|\boldsymbol{\Theta}_{\text{up}})\boldsymbol{\phi}_{\mathbf{U}}(\mathbf{u})d\mathbf{u}, \tag{7}$$

where $\bar{\cdot}$ and $\underline{\cdot}$ are the upper and lower bounds, respectively; and $\boldsymbol{\Theta}_{\text{low}}$ and $\boldsymbol{\Theta}_{\text{up}}$ are the realizations of θ that lead to the lower and upper bounds of P_f, respectively. Then, the value of β^I can be obtained based on P_f^I as follows:

$$\beta^I = \left[\underline{\beta}, \overline{\beta}\right] = \left[-\Phi^{-1}\left(\overline{P}_f\right), -\Phi^{-1}\left(\underline{P}_f\right)\right]. \tag{8}$$

As can be observed from Eqs. (6) and (8), to determine β^I and P_f^I, the key task is to find $\boldsymbol{\Theta}_{\text{low}}$ and $\boldsymbol{\Theta}_{\text{up}}$, which will be discussed in the following section.

3. Moments at the bounds of failure probability

To determine $\boldsymbol{\Theta}_{\text{low}}$ and $\boldsymbol{\Theta}_{\text{up}}$, the changing tendency of $P_f(\theta)$ with respect to θ, i.e., $\partial P_f(\theta)/\partial\theta$, needs to be investigated for $\theta \in \boldsymbol{\Theta}^I$. Denote the uncertain moments of X_i as $\theta_i = [\theta_{i1}, \theta_{i2}, \theta_{i3}] \in \boldsymbol{\theta}_i^I$, where θ_{i1}, θ_{i2} and θ_{i3} represent the uncertain mean value, standard deviation and skewness of X_i, respectively; $\boldsymbol{\theta}_i^I = [\theta_{i1}^I, \theta_{i2}^I, \theta_{i3}^I]$ is the support domain of $\boldsymbol{\theta}_i$; and $\theta_{ij}^I = \left[\underline{\theta}_{ij}, \overline{\theta}_{ij}\right]$ for $j = 1, 2, 3$, where $\underline{\theta}_{ij}$ and $\overline{\theta}_{ij}$ are the lower and upper bounds of θ_{ij}, respectively. Based on Eq. (4), $\partial P_f(\theta)/\partial\theta$ can be computed as follows:

$$\frac{\partial P_f(\theta)}{\partial \theta_{ij}} = \int_{\Omega_{\mathbf{U}}} \frac{\partial I_{\mathbf{U}}(\mathbf{u}|\theta)}{\partial \theta_{ij}} \boldsymbol{\phi}_{\mathbf{U}}(\mathbf{u})d\mathbf{u}, \quad \theta \in \boldsymbol{\Theta}^I. \tag{9}$$

Recall that, the random variables are assumed to be independent with each other in this study, and thus the value of θ_{ij} will only influence the mapping between X_i and U_i. Then, based on Eq. (5) and using the chain rule of differentiation, $\partial I_{\mathbf{U}}(\mathbf{U}|\boldsymbol{\theta})/\partial\theta_{ij}$ can be calculated as follows

$$\frac{\partial I_{\mathbf{U}}(\mathbf{U}|\boldsymbol{\theta})}{\partial\theta_{ij}} = \frac{\partial I_{\mathbf{X}}[S(\mathbf{U}|\boldsymbol{\theta})]}{\partial S(U_i|\boldsymbol{\theta}_i)} \cdot \frac{\partial S(U_i|\boldsymbol{\theta}_i)}{\partial\theta_{ij}}, \quad \theta_{ij} \in \theta_{ij}^I, \quad U_i \in \Omega_{U_i}, \tag{10}$$

where Ω_{U_i} is the domain of all possible values of U_i. Based on Eq. (2), $\partial I_{\mathbf{X}}[S(\mathbf{U}|\boldsymbol{\theta})]/\partial S(U_i|\boldsymbol{\theta}_i)$ is non-zero only for the limit state surface, i.e., $G[S(\mathbf{U}|\boldsymbol{\theta})] = 0$. Substitution of Eq. (10) into Eq. (9) leads to the reformulation of $\partial P_f(\boldsymbol{\theta})/\partial\theta_{ij}$ as follows:

$$\frac{\partial P_f(\boldsymbol{\theta})}{\partial\theta_{ij}} = \int_{G[S(\mathbf{u}|\boldsymbol{\theta})]=0} \frac{\partial I_{\mathbf{X}}[S(\mathbf{u}|\boldsymbol{\theta})]}{\partial S(u_i|\boldsymbol{\theta}_i)} \cdot \frac{\partial S(u_i|\boldsymbol{\theta}_i)}{\partial\theta_{ij}} \boldsymbol{\phi}_{\mathbf{U}}(\mathbf{u}) d\mathbf{u}, \quad \boldsymbol{\theta} \in \boldsymbol{\Theta}^I. \tag{11}$$

As $\boldsymbol{\phi}_{\mathbf{U}}(\mathbf{U})$ is always positive, the sign of $\partial P_f(\boldsymbol{\theta})/\partial\theta_{ij}$ is influenced by that of $\partial I_{\mathbf{X}}[S(\mathbf{U}|\boldsymbol{\theta})]/\partial S(U_i|\boldsymbol{\theta}_i)$ and $\partial S(U_i|\boldsymbol{\theta}_i)/\partial\theta_{ij}$. Based on the definition of indicator function in Eq. (2), the sign of $\partial I_{\mathbf{X}}[S(\mathbf{U}|\boldsymbol{\theta})]/\partial S(U_i|\theta_{ij})$ can be determined as follows:

$$\operatorname{sign}\left[\frac{\partial I_{\mathbf{X}}[S(\mathbf{U}|\boldsymbol{\theta})]}{\partial S(U_i|\boldsymbol{\theta}_i)}\right] = -\operatorname{sign}\left[\frac{\partial G(\mathbf{X})}{\partial X_i}\right]. \tag{12}$$

In this study, $G(\mathbf{X})$ is assumed to be monotonic with respect to X_i, which makes the sign of $\partial I_{\mathbf{X}}[S(\mathbf{U}|\boldsymbol{\theta})]/\partial S(U_i|\boldsymbol{\theta}_i)$ deterministic for all values of $X_i \in \Omega_{X_i}$, where Ω_{X_i} is the domain of X_i. Then, the key task to determine the sign of $\partial I_{\mathbf{U}}(\mathbf{U}|\boldsymbol{\theta})/\partial\theta_{ij}$ as well as that of $\partial P_f(\boldsymbol{\theta})/\partial\theta_{ij}$ is to determine the sign of $\partial S(U_i|\boldsymbol{\theta}_i)/\partial\theta_{ij}$ for all possible values of $U_i \in \Omega_{U_i}$, which will be addressed in the following.

3.1. Changing tendency of inverse normal transformation with moments

In this section, $\partial S(U_i|\boldsymbol{\theta}_i)/\partial\theta_{ij}$ will be analyzed considering uncertainties in all the first three moments of X_i. The consideration of the first three moments is motivated by the importance of the third moment (skewness) in characterizing the asymmetry of a random variable's distribution, which is crucial for a general reliability analysis [19,20]. Note that, other cases with less uncertain moments are reduced cases of the considered one. Given the value of U_i, $X_i = S(U_i|\boldsymbol{\theta}_i)$ is obtained via inverse normal transformation. In this study, the distribution of X_i is simulated based on the first three moments with the aid of squared normal distribution [19], which is proved to be flexible to represent a large number of general distributions. Following this, X_i can be expressed by a quadratic polynomial of $U_i \in \Omega_{X_i}$ and $\boldsymbol{\theta}_i \in \boldsymbol{\theta}_i^I$ as follows [19]:

$$X_i = S(U_i|\boldsymbol{\theta}_i) = \theta_{i1} + \theta_{i2}[a_1(\theta_{i3})U_i^2 + a_2(\theta_{i3})U_i + a_3(\theta_{i3})], \tag{13}$$

where $a_1(\theta_{i3})$, $a_2(\theta_{i3})$ and $a_3(\theta_{i3})$ are parameters determined by the skewness θ_{i3} as follows [21]:

$$a_1(\theta_{i3}) = \frac{\sqrt{3}}{10}\theta_{i3}, \quad a_2(\theta_{i3}) = 1 - \frac{\sqrt{3}}{50}\theta_{i3}^2, \quad a_3(\theta_{i3}) = -\frac{\sqrt{3}}{10}\theta_{i3}. \tag{14}$$

Based on Eqs. (13) and (14), $\partial S(U_i|\boldsymbol{\theta}_i)/\partial\theta_{ij}$ can be obtained, and its sign will be discussed in the following.

(1) Sign of $\partial S(U_i|\boldsymbol{\theta}_i)/\partial\theta_{i1}$

Based on Eqs. (13) and (14), $\partial S(U_i|\boldsymbol{\theta}_i)/\partial\theta_{i1}$ is calculated as follows:

$$\frac{\partial S(U_i|\boldsymbol{\theta}_i)}{\partial\theta_{i1}} = 1. \tag{15}$$

Based on Eq. (15), $\partial S(U_i|\boldsymbol{\theta}_i)/\partial\theta_{i1}$ is always positive. This indicates that, when $G(\mathbf{X})$ is monotonic with respect to X_i, it is possible to determine the values of θ_{i1} that minimize and maximize the failure probability.

(2) Sign of $\partial S(U_i|\boldsymbol{\theta}_i)/\partial\theta_{i2}$

Based on Eqs. (13) and (14), $\partial S(U_i|\boldsymbol{\theta}_i)/\partial\theta_{i2}$ is calculated as follows:

$$\frac{\partial S(U_i|\boldsymbol{\theta}_i)}{\partial\theta_{i2}} = a_1(\theta_{i3})U_i^2 + a_2(\theta_{i3})U_i + a_3(\theta_{i3}). \tag{16}$$

Eqs. (14) and (16) reveal that, the sign of $\partial S(U_i|\boldsymbol{\theta}_i)/\partial\theta_{i2}$ is determined by U_i and θ_{i3}. Although the value of skewness is uncertain, its sign is typically known in practical engineering. Then, the sign of $\partial S(U_i|\boldsymbol{\theta}_i)/\partial\theta_{i2}$ can be determined for skewness with different signs.

(a) When $\theta_{i3} = 0$, the sign of $\partial S(U_i|\boldsymbol{\theta}_i)/\partial\theta_{i2}$ is only determined by U_i as follows:

$$\operatorname{sign}\left[\frac{\partial S(U_i|\boldsymbol{\theta}_i)}{\partial\theta_{i2}}\right] = \operatorname{sign}(U_i), \tag{17}$$

When $\theta_{i3} \neq 0$, the key to determining the sign of $\partial S(U_i|\boldsymbol{\theta}_i)/\partial\theta_{i2}$ is to find the root of the equation $\partial S(U_i|\boldsymbol{\theta}_i)/\partial\theta_{i2} = 0$ with respect to U_i in terms of θ_{i3}. Based on Eq. (16), the roots can be obtained as follows:

$$p = \frac{-50 + \sqrt{3}\theta_{i3}^2}{10\sqrt{3}\theta_{i3}} - \frac{\sqrt{2500 + 300\theta_{i3}^2 - 100\sqrt{3}\theta_{i3}^2 + 3\theta_{i3}^4}}{10\sqrt{3}|\theta_{i3}|}, \tag{18}$$

$$q = \frac{-50 + \sqrt{3}\theta_{i3}^2}{10\sqrt{3}\theta_{i3}} + \frac{\sqrt{2500 + 300\theta_{i3}^2 - 100\sqrt{3}\theta_{i3}^2 + 3\theta_{i3}^4}}{10\sqrt{3}|\theta_{i3}|}. \tag{19}$$

For practical engineering reliability problems, $|\theta_{i3}|$ is relatively small (less than 2), and p and q can be simplified as follows:

$$p = \frac{-5}{\sqrt{3}\theta_{i3}} - \frac{5}{\sqrt{3}|\theta_{i3}|}, \quad q = \frac{-5}{\sqrt{3}\theta_{i3}} + \frac{5}{\sqrt{3}|\theta_{i3}|}. \tag{20}$$

(b) When $\theta_{i3} < 0$, the sign of $\partial S(U_i|\boldsymbol{\theta}_i)/\partial\theta_{i2}$ is determined by U_i and θ_{i3} as follows:

$$\begin{cases} \dfrac{\partial S(U_i|\boldsymbol{\theta}_i)}{\partial\theta_{i2}} < 0, & U_i \in (-\infty, p) \cup (q, +\infty) \\ \dfrac{\partial S(U_i|\boldsymbol{\theta}_i)}{\partial\theta_{i2}} \geq 0, & U_i \in [p, q] \end{cases}, \tag{21}$$

To obtain the reliable bounds for the failure probability when the skewness is uncertain but known to be negative, based on Eq. (20), p and q are further expressed as follows:

$$p = 0, \quad q = \frac{1}{a_3(\overline{\theta}_{i3})}. \tag{22}$$

(c) When $\theta_{i3} > 0$, the sign of $\partial S(U_i|\boldsymbol{\theta}_i)/\partial\theta_{i2}$ is determined by U_i and θ_{i3} as follows:

$$\begin{cases} \dfrac{\partial S(U_i|\boldsymbol{\theta}_i)}{\partial\theta_{i2}} < 0, & U_i \in [p, q] \\ \dfrac{\partial S(U_i|\boldsymbol{\theta}_i)}{\partial\theta_{i2}} \geq 0, & U_i \in (-\infty, p) \cup (q, +\infty) \end{cases}, \tag{23}$$

Based on Eq. (20), when the skewness is uncertain but known to be positive, p and q are formulated as follows:

$$p = \frac{1}{a_3(\underline{\theta}_{i3})}, \quad q = 0. \tag{24}$$

(3) Sign of $\partial S(U_i|\boldsymbol{\theta}_i)/\partial\theta_{i3}$

Based on Eqs. (13) and (14), $\partial S(U_i|\boldsymbol{\theta}_i)/\partial\theta_{i3}$ can be obtained as follows:

$$\frac{\partial S(U_i|\boldsymbol{\theta}_i)}{\partial\theta_{i3}} = \frac{\sqrt{3}}{50}\theta_{i2}\left(5U_i^2 - 2\theta_{i3}U_i - 5\right), \tag{25}$$

Based on Eqs. (25), the sign of $\partial U_i/\partial\theta_{i3}$ can be determined by U_i and θ_{i3} as follows:

$$\begin{cases} \dfrac{\partial S(u_i|\boldsymbol{\theta}_i)}{\partial\theta_{i3}} < 0, & U_i \in [a, b] \\ \dfrac{\partial S(u_i|\boldsymbol{\theta}_i)}{\partial\theta_{i3}} \geq 0, & U_i \in (-\infty, a) \cup (b, +\infty) \end{cases}, \tag{26}$$

where a and b are computed as follows:

$$a = \frac{\theta_{i3} - \sqrt{25 + \theta_{i3}^2}}{5}, \quad b = \frac{\theta_{i3} + \sqrt{25 + \theta_{i3}^2}}{5}. \tag{27}$$

For practical case with $|\theta_{i3}| \leq 2$, the values of a and b slightly fluctuate around -1 and 1, respectively. These slight fluctuations have negligible effects on the sign of $\partial U_i/\partial\theta_{i3}$, thus a and b can be approximated as -1 and 1, respectively.

To sum up, the values of θ_{i1} at the bounds of $P_f(\boldsymbol{\theta})$ can be determined for all possible values of $X_i \in \Omega_{X_i}$, while those of θ_{i2} and θ_{i3} can only be obtained for specific value of U_i. As the values of θ_{i2} and θ_{i3} may be different for different values of U_i, it may happen that the distribution of corresponding X_i at the bounds of failure probability is modeled by a set of different moments. This does not satisfy the constraints that, each random variable has only one set of moments when calculating the failure probability as a function of those moments. If such constraints are lifted, the bounds of failure probability obtained will be conservative when compared to the actual ones. That is, the proposed approach approximates the failure probability bounds with a conservative interval. However, as the failure probability is evaluated at the tails of random variables, where there is generally only one set of moments driving the sign of $\partial P_f(\boldsymbol{\theta})/\theta_{ij}$, the corresponding bounds of failure probability are relatively tight.

3.2. Values of uncertain moments at the bounds of failure probability

As discussed above, for the case when random variables are independent with each other, the sign of $\partial P_f(\boldsymbol{\theta})/\partial\theta_{ij}$ with $\theta_{ij} \in \theta_{ij}^I$ can be determined based on the value of U_i and the sign of $\partial G(\mathbf{X})/\partial X_i$. Then, the value of θ_{ij} for the bounds of $P_f(\boldsymbol{\theta})$ can be determined accordingly: When $\partial P_f(\boldsymbol{\theta})/\partial\theta_{ij} \leq 0$, $P_f(\boldsymbol{\theta})$ decreases with θ_{ij}, indicating the values of θ_{ij} for the lower and upper bounds of $P_f(\boldsymbol{\theta})$ should be $\overline{\theta}_{ij}$ and $\underline{\theta}_{ij}$, respectively; When $\partial P_f(\boldsymbol{\theta})/\partial\theta_{ij} > 0$, $P_f(\boldsymbol{\theta})$ increases with θ_{ij}, and the values of θ_{ij} for the lower and upper bounds of $P_f(\boldsymbol{\theta})$ should be $\underline{\theta}_{ij}$ and $\overline{\theta}_{ij}$, respectively. For application, the values of uncertain moments for different combinations of U_i and $\partial G(\mathbf{X})/\partial X_i$ are summarized in Table 1.

Table 1
Values of uncertain moments for inverse normal transformation.

Uncertain moment	$\frac{\partial G(\mathbf{X})}{\partial X_i}$	U_i		$\boldsymbol{\Theta}_{\text{low}}$	$\boldsymbol{\Theta}_{\text{up}}$
		$\theta_{i3} \le 0$	$\theta_{i3} > 0$		
θ_{i1}	< 0	$(-\infty, +\infty)$		$\underline{\theta}_{i1}$	$\overline{\theta}_{i1}$
	≥ 0			$\overline{\theta}_{i1}$	$\underline{\theta}_{i1}$
θ_{i2}	< 0	$(-\infty, 0) \cup (q, +\infty)$	$[p, 0]$	$\overline{\theta}_{i2}$	$\underline{\theta}_{i2}$
		$[0, q]$	$(-\infty, p) \cup (0, +\infty)$	$\underline{\theta}_{i2}$	$\overline{\theta}_{i2}$
	≥ 0	$(-\infty, 0) \cup (q, +\infty)$	$[p, 0]$	$\underline{\theta}_{i2}$	$\overline{\theta}_{i2}$
		$[0, q]$	$(-\infty, p) \cup (0, +\infty)$	$\overline{\theta}_{i2}$	$\underline{\theta}_{i2}$
θ_{i3}	< 0	$(-\infty, -1)$	$(1, +\infty)$	$\underline{\theta}_{i3}$	$\overline{\theta}_{i3}$
		$[-1, 0]$	$[0, 1]$	$\overline{\theta}_{i3}$	$\underline{\theta}_{i3}$
	≥ 0	$(-\infty, -1)$	$(1, +\infty)$	$\overline{\theta}_{i3}$	$\underline{\theta}_{i3}$
		$[-1, 0]$	$[0, 1]$	$\underline{\theta}_{i3}$	$\overline{\theta}_{i3}$

4. Procedure and efficiency of TIPP method

With $\boldsymbol{\Theta}_{\text{low}}$ and $\boldsymbol{\Theta}_{\text{up}}$ determined using Table 1, the parametric p-boxes can be replaced by general distributions for the bounds of failure probability. And then, P_f^I and β^I can be computed using classical reliability analysis methods, such as the first-order reliability method (FORM) [22,23], the second-order reliability method (SORM) [24,25], the method of moments (MoM) [26] and the method of moments combined with control variates (MoM-CV) [27]. Additionally, various sampling-based techniques can be applied, such as Monte Carlo simulation (MCS), subset simulation (SS), importance sampling, and other advanced sampling methods. For different problems, appropriate methods can be flexibly combined according to the specific requirements, highlighting the flexibility of TIPP method.

The procedure of TIPP method is summarized in Fig. 2, and further details of three main steps summarized as follows:

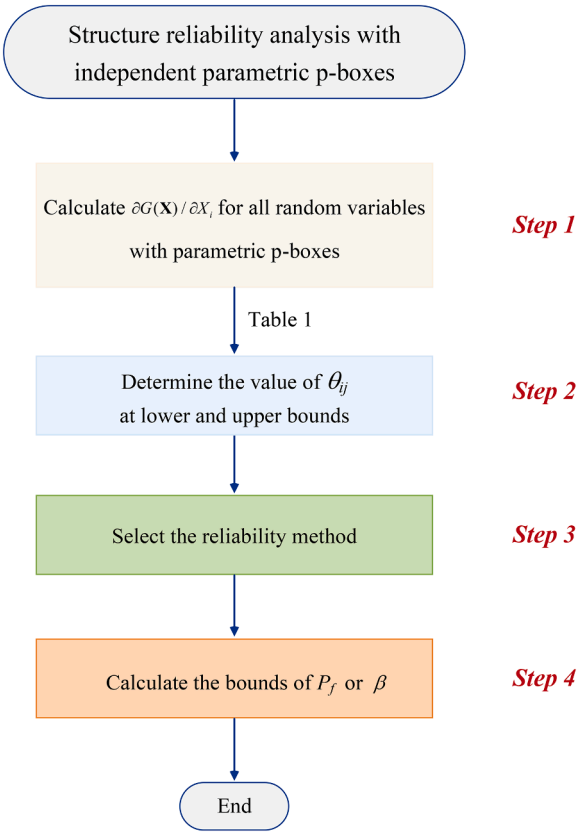

Fig. 2. Procedure of TIPP method.

(1) Determine the sign of $\partial G(\mathbf{X})/\partial X_i$ for all random variables with parametric p-boxes. When $G(\mathbf{X})$ is implicit, the finite differences method can be applied to evaluate $\partial G(\mathbf{X})/\partial X_i$. Note that TIPP method is developed for the case when $G(\mathbf{X})$ is monotonic with respect to X_i, the sign of $\partial G(\mathbf{X})/\partial X_i$ should remain the same for all possible values of X_i.
(2) Determine the value of θ_{ij} at lower and upper bounds. The determination of $\boldsymbol{\Theta}_{\text{low}}$ and $\boldsymbol{\Theta}_{\text{up}}$ for X_i can be conducted as follows:
   - Determine the value of θ_{i1} using $\partial G(\mathbf{X})/\partial X_i$.
   - Determine the values of θ_{i2} at the bounds, which are conditioned on the value of U_i.
   - Determine the values of θ_{i3} at the bounds, which are conditioned on the value of U_i.
(3) Select the reliability method. The selection of the reliability method is contingent upon the characteristics of the performance function. When the performance function is simple and differentiable, FORM or SORM can be employed. The choice between them is guided by the curvature radius of the performance function. Specifically, FORM is selected when the average curvature radius of the performance function in Gaussian space, denoted as R, satisfies the following condition [28]:

$$|R| \geq (m-1)/(2\varepsilon_a \beta_{\text{FORM}}), \tag{28}$$

where $|R|$ is the absolute value of R; m is the dimension of random variables; ε_a is the allowable error; and β_{FORM} is the reliability index obtained by FORM. Conversely, when the inequality in Eq. (28) does not hold, SORM should be employed for a more accurate estimation.

For problems involving a complex, implicit, or highly non-linear performance function where even SORM may be inaccurate, the Method of Moments (MoM) is employed. Nonetheless, the conventional MoM itself faces challenges with the "curse of dimensionality," as its efficiency deteriorates in very high-dimensional problems (see Section A.3). To overcome this problem, the MoM-CV is employed as a more efficient alternative in such cases.
(4) Calculate P_f^I and β^I. This is achieved by conducting two times of reliability analyses based on $\boldsymbol{\Theta}_{\text{low}}$ and $\boldsymbol{\Theta}_{\text{up}}$. In each reliability analysis, either $\boldsymbol{\Theta}_{\text{low}}$ or $\boldsymbol{\Theta}_{\text{up}}$ is applied to define the inverse normal transformation, i.e., $X_i = S(U_i|\boldsymbol{\theta}_i)$.

The efficiency of the proposed TIPP method can be evaluated based on the number of performance function evaluations required. As discussed above, before estimation of P_f^I and β^I, $\partial G(\mathbf{X})/\partial X_i$ needs to be calculated for all random variables characterized by parametric p-boxes. In this step, the number of performance function evaluations is either equal to one (in case that the performance function and its derivatives are available analytically) or, for implicit performance functions available as black-boxes, the number of parametric p-boxes plus one. Once $\partial G(\mathbf{X})/\partial X_i$ is obtained, there is no evaluation of performance functions required for determining $\boldsymbol{\Theta}_{\text{low}}$ and $\boldsymbol{\Theta}_{\text{up}}$. Following this, only two classical reliability analyses are needed, and the number of performance function evaluations depends on the reliability method adopted. As the number of parametric p-boxes is no larger than that of $\mathbf{X}$, which is no more than the number of performance function evaluations for a single reliability analysis, the number of performance function evaluations required by the TIPP method is always less than that required for three times of reliability analyses. This underscores the efficiency and broad applicability of TIPP method.

5. Illustrative examples

To investigate the application of the proposed TIPP method for reliability analysis considering parametric p-boxes, four examples are considered in this section. The first example considers a mathematical problem with analytical solution, which is adopted to examine the accuracy of TIPP method. The second example evaluates the efficiency of TIPP method using a truss model that considers 14 uncertain distribution parameters. The third example involves two-degree-of-freedom primary-secondary damped oscillator with a highly nonlinear performance function considering the uncertainty of skewness, to demonstrate the applicability of TIPP method for highly nonlinear problems. The final example is a seepage problem with implicit performance function, which effectively demonstrates the practical applicability and computational efficiency of TIPP method in handling complex engineering problems. All scripts are coded with Mathematica 11.3 and MATLAB R2024a and run on a computer with Intel(R) Core(TM) i7-12700U CPU @ 2.30 GHz and RAM 16G.

5.1. Example 1: Mathematical problem

Consider a linear performance function with two independent random variables as follows:

$$G(\mathbf{X}) = X_1 - X_2, \tag{29}$$

where X_1 and X_2 are two parameters, which are assumed to be independent normally distributed parametric p-boxes, with $\theta_{11} = [390, 410]$, $\theta_{21} = [250, 270]$, $\theta_{12} = [19.5, 20.5]$, and $\theta_{22} = [38.5, 39.5]$. These parameters are adopted from Table 1 of Ref. [29].

For this simple example, analytical solutions to β^I and P_f^I exist as follows [12]:

$$\beta^I = \left[\underline{\beta}, \overline{\beta}\right] = \left[\frac{\underline{\theta}_{11} - \overline{\theta}_{21}}{\sqrt{\left(\overline{\theta}_{12}\right)^2 + \left(\overline{\theta}_{22}\right)^2}}, \frac{\overline{\theta}_{11} - \underline{\theta}_{21}}{\sqrt{\left(\underline{\theta}_{12}\right)^2 + \left(\underline{\theta}_{22}\right)^2}}\right], \tag{30}$$

Table 2
First two moments in the lower and upper bounds for Example 1.

Uncertain moment	Range of U_i	$\boldsymbol{\Theta}_{\text{low}}$	$\boldsymbol{\Theta}_{\text{up}}$
θ_{11}	$(-\infty,+\infty)$	410	390
θ_{12}	$(-\infty,0)$	19.5	20.5
	$[0,+\infty)$	20.5	19.5
θ_{21}	$(-\infty,+\infty)$	250	270
θ_{22}	$(-\infty,0)$	39.5	38.5
	$[0,+\infty)$	38.5	39.5

Table 3
Reliability analysis results for Example 1.

Method	Reliability index β				Function evaluation	Time (s)
	Lower bound		Upper bound			
	Value	R.E. (%)	Value	R.E. (%)		
Analytical solution	2.6965	–	3.7074	–	–	–
BU-BDRM-Kriging [29]	2.6685	1.04	3.6375	1.89	25	56
TIPP-FORM	2.6965	–	3.7074	–	6	0.12
TIPP-SORM	2.6965	–	3.7074	–	8	0.42
TIPP-MoM	2.6870	0.35	3.7399	0.88	52	0.02

$$P_f^I = \left[\Phi\left(-\overline{\beta}\right), \Phi\left(-\underline{\beta}\right)\right] = \left[\Phi\left(-\frac{\overline{\theta}_{11} - \underline{\theta}_{21}}{\sqrt{\left(\underline{\theta}_{12}\right)^2 + \left(\underline{\theta}_{22}\right)^2}}\right), \Phi\left(-\frac{\underline{\theta}_{11} - \overline{\theta}_{21}}{\sqrt{\left(\overline{\theta}_{12}\right)^2 + \left(\overline{\theta}_{22}\right)^2}}\right)\right]. \tag{31}$$

In this example, the derivatives of the performance function with respect to these random variables are calculated as

$$\frac{\partial G(\mathbf{X})}{\partial X_1} = 1, \quad \frac{\partial G(\mathbf{X})}{\partial X_2} = -1\,. \tag{32}$$

The sign of $\partial G(\mathbf{X})/\partial X_1$ is positive, and the sign of $\partial G(\mathbf{X})/\partial X_2$ is negative. Thus, $\boldsymbol{\Theta}_{\text{low}}$ and $\boldsymbol{\Theta}_{\text{up}}$ can be constructed based on Table 1, which are listed in Table 2.

Then, the interval of reliability index, i.e., β^I, can be calculated. Based on Eqs. (30) and (31), the analytical solution to β^I is obtained as [2.6965, 3.7074]. For comparison, the example is also investigated using the proposed TIPP method, with the reliability analysis conducted by FORM, SORM and method of moments. Additionally, the Bayesian updating Bivariate Dimension Reduction Method (BDRM) with Kriging surrogate model, commonly referred to as BU-BDRM-Kriging method [29], whose results are adopted from Table 2 of Ref. [29], is also employed.

The values of β^I evaluated by different methods are compared in Table 3, along with the relative error (denoted by R.E.) compared with analytical results. It is found that, the results of TIPP method combined with FORM/SORM can obtain exact evaluation of β^I, while the results from TIPP method combined with method of moments and BU-BDRM-Kriging have a relatively small R.E. within 5%.

The results presented in Table 3 demonstrate that TIPP method provides a more precise estimation for both the lower and upper bounds of the reliability index compared with BU-BDRM-Kriging method. While the BU-BDRM-Kriging method requires 25 function evaluations, this is still greater than the number required by TIPP-FORM and TIPP-SORM. Additionally, due to the sampling and optimization procedure involved in constructing BU-BDRM-Kriging method, its computational time is considerably higher than that of any of TIPP methods. These comparisons emphasize the advantage of TIPP method in achieving both accuracy and efficiency when evaluating the bounds of the reliability index.

Additionally, to assess the impact of the approximation of piece-wise distribution of random variables in TIPP method on the results, Fig. 3 presents the piece-wise LSFs used in TIPP method, along with the exact upper and lower bounds of the LSF corresponding to Eqs. (30) and (31). Further more, Fig. 3 shows potential LSFs corresponding to various combinations of the bounds of uncertain moments. As observed in Fig. 3, the approximated LSFs applied in TIPP method define the outermost boundary of all possible LSFs while remaining closely aligned with the exact ones. This explains why TIPP method provides a tight yet broader approximation of the reliability index and failure probability bounds. Notably, the approximated LSFs in TIPP method coincide with the exact ones near the region close to the origin, resulting in an accurate evaluation of β^I when using TIPP method combined with FORM/SORM, which seeks the shortest distance from the origin to the LSF. In the method of moments, the moments of the performance function are used in the reliability evaluation and are estimated based on the entire LSF. Consequently, any relative error in the approximated LSF in other regions leads to a corresponding relative error in the calculated β^I.

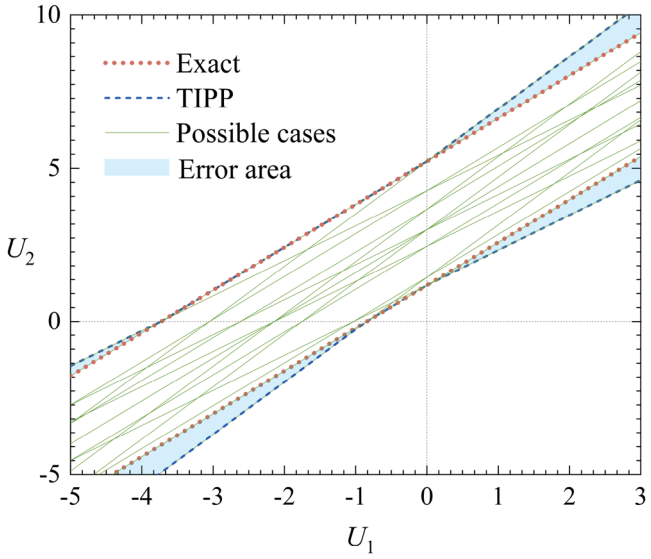

Fig. 3. Lower and upper bounds of limit state functions for Example 1.

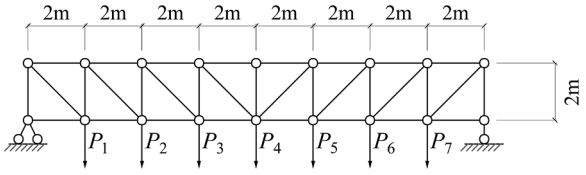

Fig. 4. The schematic diagram of truss model for Example 2.

Table 4
Reliability analysis results for Example 2.

Method	Reliability index β				Function evaluation	Time (s)
	Lower bound		Upper bound			
	Value	R.E. (%)	Value	R.E. (%)		
Double loop MCS	1.3613	–	3.4357	–	8247758199	27263
BU-BDRM-Kriging [29]	1.3278	2.46	3.3686	1.95	365	35
TIPP-FORM	1.5652	14.98	3.5936	4.60	15	1.24
TIPP-SORM	1.5664	15.07	3.5202	2.46	21	2.73
TIPP-MoM	1.3397	1.59	3.4830	1.38	737	0.05

5.2. Example 2: Truss structure

A truss modified from Ref. [30] is investigated, as shown in Fig. 4. Considering the vertical displacement at the truss middle point should be less than the requirement of vertical displacement δ_s, the performance function is constructed as:

$$G(\mathbf{X}) = \delta_s - \delta, \tag{33}$$

where δ_s is set to be 0.029 m; and δ is the vertical displacement at the truss middle point. The modulus of elasticity of the material is 200×10^9 Pa, and the cross-sectional area of the bar element is 0.005 35 m^2. The seven loads are independent lognormal variables with mean in the range 95 kN to 105 kN and standard deviation in the range 13 kN to 17 kN. Thus, in this example, 7 parametric p-boxes are considered, with 14 uncertain moments.

Again, the bounds of reliability index are calculated using the proposed TIPP method and double-loop MCS. The results of reliability index and function evaluations calculated by different methods are compared in Table 4. It can be observed from Table 4 that, the relative difference between the results of TIPP method combined with the method of moments and those from MCS remains under 3%, demonstrating the accuracy of TIPP method. However, it is worth noting that the results from TIPP method combined with FORM/SORM exhibit relatively larger relative errors, which can be attributed to the nonlinearity of the performance function. Therefore, it is recommended to choose an appropriate reliability analysis method based on the specific problem.

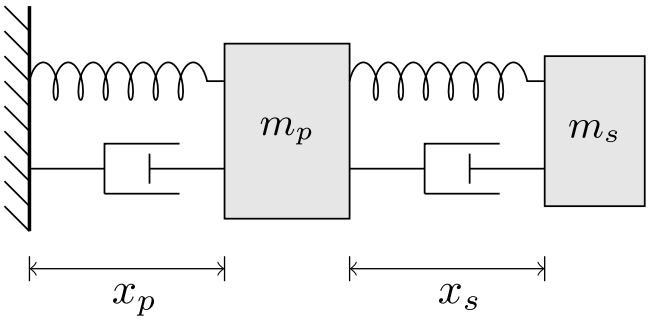

Fig. 5. The schematic diagram of two-degree-of-freedom primary-secondary damped oscillator.

Table 5
The probabilistic information for Example 3.

Random Variable	Mean	Standard Deviation	Skewness	Distribution
k_p (N/m)	1.000	0.200	0.400	Gamma
k_s (N/m)	0.010	0.002	0.400	Gamma
ζ_p	0.050	0.005	0.301	Lognormal
ζ_s	0.020	0.002	0.301	Lognormal
F_s (N)	[15.000, 18.000]	[0.100, 0.200]	[0.200, 0.400]	Unknown
S_0 (m^2/s^3)	[90.000, 110.000]	[5.000, 15.000]	[0.100, 0.500]	Unknown

From the aspect of efficiency, the number of performance function evaluations required by the proposed TIPP method is much smaller than that of the double-loop MCS. Moreover, the computational time of TIPP-MoM remains nearly constant for examples 1 and 2, even as the number of uncertain moments increases from 4 to 14. This consistency is due to the absence of optimization in TIPP method, making its efficiency unaffected by the number of uncertain distribution parameters.

5.3. Example 3: Two-degree-of-freedom primary-secondary damped oscillator

The third example considers a two-degree-of-freedom primary-secondary damped oscillator, which is adopted from Refs. [31] and shown in Fig. 5. The primary-secondary damped oscillator is characterized by the masses m_p and m_s, spring stiffnesses k_p and k_s, damping ratios ζ_p and ζ_s, and natural frequencies $\omega_p = (k_p/m_p)^{1/2}$ and $\omega_s = (k_s/m_s)^{1/2}$. The subscripts p and s respectively refer to the primary and secondary oscillators.

With a white-noise base excitation, the performance function is expressed as follows [32]:

$$G(\mathbf{X}) = F_s - 3k_s\sqrt{\frac{\pi S_0}{4\zeta_s\omega_s^3}\left[\frac{\zeta_a\zeta_s}{\zeta_p\zeta_s(4\zeta_a^2+\theta_{sr}^2)+\gamma\zeta_a^2}\frac{(\zeta_p\omega_p^3+\zeta_s\omega_s^3)\omega_p}{4\zeta_a\omega_a^4}\right]}, \tag{34}$$

where F_s denotes the force capacity of the secondary spring; S_0 denotes the intensity of the white noise; $\gamma = m_s/m_p$ denotes the mass ratio; $\omega_a = (\omega_p + \omega_s)/2$ denotes the average frequency; $\zeta_a = (\zeta_p + \zeta_s)/2$ denotes the damping ratio; and $\theta_{sr} = (\omega_p - \omega_s)/\omega_a$ denotes a tuning parameter.

In this example, the mass parameters m_p and m_s are set to 1 kg and 0.01 kg, respectively. Table 5 summarizes the probabilistic information of all random variables involved. Based on Table 7 in Ref. [31], this example additionally considers uncertainties in the statistical moments and distribution types for F_s and S_0.

The bounds of reliability index are calculated using double-loop MCS and the proposed TIPP method. As the distributions of the random variables are unknown, the third-moment normal transformation technique is applied for generating random variables in MCS as given in Eq. (13) [19].

The results obtained from MCS, BU-BDRM-Kriging method and TIPP method are compared in Table 6, which shows that the reliability index computed by TIPP-MoM are in closer agreement with those obtained from MCS with relative error less than 1 %, while the relative error of the results calculated by TIPP-FORM exceeds 20 %. For this strongly nonlinear performance function, the limitations of the FORM approach lead to the inaccuracy of TIPP-FORM for such complex problems. Furthermore, it is noteworthy that TIPP-MoM achieves the highest accuracy with computational time significantly less than that required by other methods, demonstrating its efficiency for practical engineering with the strong nonlinear performance functions.

5.4. Example 4: Seepage problem below a dam

The last example involves the study of a steady state confined seepage below a dam, adapted from Ref. [33] and shown in Fig. 6(a). To avoid the failure event caused by the seepage discharge below the dam exceeding a threshold, the performance function is given

Table 6
Reliability analysis results for Example 3.

Method	Reliability index β				Function evaluation	Time (s)
	Lower bound		Upper bound			
	Value	R.E. (%)	Value	R.E. (%)		
Double loop MCS	3.5763	–	4.8962	–	180679595	3305
BU-BDRM-Kriging [29]	3.5320	1.24	4.8285	1.38	265	46
TIPP-FORM	5.0612	41.52	6.3528	29.75	18	1.54
TIPP-SORM	3.6181	1.17	4.9888	1.89	118	11.64
TIPP-MoM	3.5681	0.23	4.9460	1.02	532	0.15

Table 7
The probabilistic information for Example 4.

Random Variable	Mean	Standard Deviation
$k_{xx,1}$(m/s)	$[5.5, 6.0] \times 10^{-7}$	$[3, 6] \times 10^{-8}$
$k_{yy,1}$(m/s)	$[2.3, 2.6] \times 10^{-7}$	$[4, 5] \times 10^{-8}$
$k_{xx,2}$(m/s)	$[5.5, 6.0] \times 10^{-6}$	$[3, 6] \times 10^{-7}$
$k_{yy,2}$(m/s)	$[2.3, 2.6] \times 10^{-6}$	$[4, 5] \times 10^{-7}$

Table 8
Reliability analysis results for Example 4.

Method	Reliability index β				Function evaluation	Time (s)
	Lower bound		Upper bound			
	Value	R.E. (%)	Value	R.E. (%)		
Double loop MCS	1.8857	–	4.4652	–	47122645	38263
BU-BDRM-Kriging [29]	1.8531	1.73	4.3814	1.88	113	102
TIPP-MoM	1.8700	0.83	4.4907	0.57	226	10.58

as follows:

$$G(\mathbf{X}) = q_0 - q, \tag{35}$$

where q_0 is set to be 2×10^{-6} m^3/s. The seepage discharge q is computed per unit width of the dam and measured in units of volume over time and distance, which can be calculated as follows:

$$q = -\int_{\mathrm{CD}} k_{yy,2} \frac{\partial h_W}{\partial y} dx, \tag{36}$$

where CD represents the downstream side of the dam as shown in Fig 6(a); $k_{yy,2}$ is the vertical permeability of the second soil layer; and h_W is the hydraulic head, which is solved by the following equation:

$$k_{xx,i} \frac{\partial^2 h_W}{\partial x^2} + k_{yy,i} \frac{\partial^2 h_W}{\partial y^2} = 0, \quad i = 1, 2, \tag{37}$$

where $k_{xx,i}$ and $k_{yy,i}$ represent the horizontal and vertical permeabilities of the ith soil layer, respectively; and x and y denote horizontal and vertical coordinates, respectively. The boundary conditions for this equation are that: (1) h_W over segments AB and CD is $20 + h_D$ m and 20 m, respectively, where $h_D = 8$ m is the height of water; (2) there is null flow over other boundaries. This equation is solved numerically using the finite element (FE) method (see, e.g. Ref. [34]), which is modeled by MATLAB R2024a. As illustrate in Fig. 6(b), the FE model consists 1258 nodes and 1628 quadratic triangular elements. The permeabilities, i.e., $k_{xx,i}$ and $k_{yy,i}$ are considered as lognormally distributed random variables with independent parametric p-boxes, with their parameters adopted from Table 1 of Ref. [33] and statistical information summarized in Table 7.

Considering the physics of this problem, where an increase in permeability value leads to increased seepage discharge and failure probability, the proposed TIPP method is applicable. Double-loop Monte Carlo simulation (MCS) is adopted to examine the accuracy of TIPP method. The outer loop is simulated with 10^8 samples, and the inner loop searches for the maximum and minimum values of the performance function for different uncertain moments using Fmincon Optimization.

The results obtained from MCS, BU-BDRM-Kriging method and TIPP method are compared in Table 8, which shows that the reliability indices computed by BU-BDRM-Kriging method and TIPP method are in close agreement with those obtained from MCS with relative errors less than 5 %. Although BU-BDRM-Kriging method requires fewer function evaluations than TIPP-MoM, the computational time of TIPP-MoM is significantly shorter while simultaneously providing more accurate results. This computational advantage highlights the efficiency of TIPP-MoM for practical engineering applications. This example, featuring an implicit performance function and a potentially small failure probability problem, further validates the potential prospects of TIPP method for practical engineering applications.

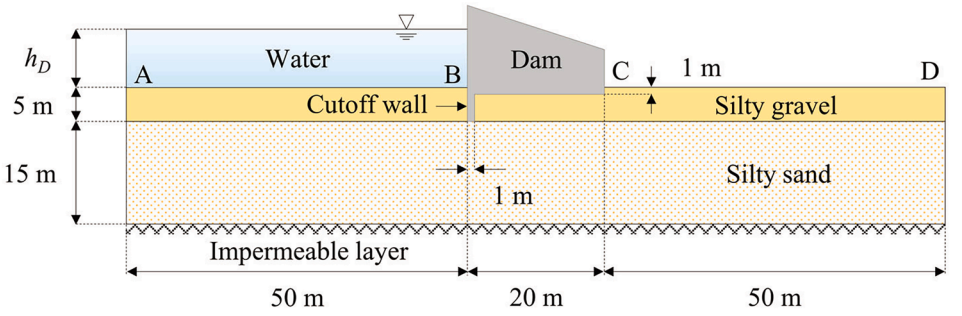

(a) The schematic diagram of seepage problem below a dam

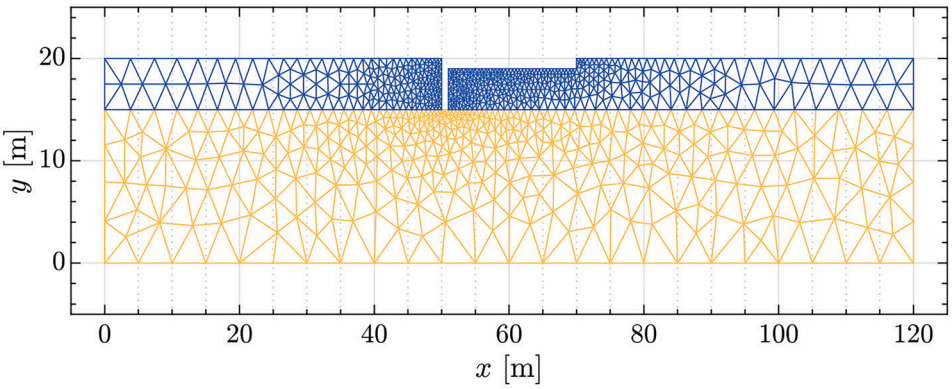

(b) The FE model mesh for seepage problem below a dam

Fig. 6. Seepage problem below a dam: (a) schematic diagram and (b) FE model mesh.

6. Conclusions

TIPP method is proposed for reliability analysis involving independent parametric p-boxes, under the assumption that the performance function is monotonic with respect to random variables modeled by parametric p-boxes. Epistemic uncertainties are incorporated by considering the first three moments and modeling them as interval variables. Based on the derivative of the performance function with respect to the random variables modeled by parametric p-boxes, the values of uncertain moments can be directly determined for calculating the bounds of failure probability in TIPP method, thus eliminating the need for optimization.

The application of TIPP method is investigated through four examples incorporated with a large number of uncertain statistical moments, strongly nonlinear problem and implicit performance function. These examples show that the proposed TIPP method can efficiently calculate the bounds of failure probability, which are in close agreement with those obtained through double-loop MCS. The proposed method exhibits minimal computational time even with a FE model, and the efficiency of the proposed TIPP method is irrelevant to the number of uncertain statistical moments. In summary, TIPP method demonstrates excellent applicability to practical engineering problems with implicit and nonlinear performance functions, offering both high accuracy and significant computational efficiency advantages.

Despite the demonstrated effectiveness of TIPP method in various examples, certain limitations remain that should be acknowledged. A primary limitation of TIPP method is the requirement that the performance function be monotonic with respect to random variables characterized by uncertain moments. To address this, a key direction for future work is to integrate an approximate method. Other challenges to be addressed include extending the method to handle correlated random variables and improving its performance for strongly non-Gaussian problems with extremely small failure probabilities.

CRediT authorship contribution statement

Bo-Yu Wang: Writing – review & editing, Writing – original draft, Visualization, Validation, Software, Methodology, Conceptualization; **Xuan-Yi Zhang:** Writing – review & editing, Visualization, Funding acquisition, Conceptualization; **Yan-Gang Zhao:** Writing – review & editing, Supervision, Funding acquisition; **Marcos A. Valdebenito:** Writing – review & editing; **Matthias G.R. Faes:** Writing – review & editing, Supervision, Funding acquisition.

Data availability

Data will be made available on request.

Declaration of competing interest

The authors declare that they have no known competing financial interests or personal relationships that could have appeared to influence the work reported in this paper.

Acknowledgment

The study is partially supported by the National Key R&D Program of China (Grant No. 2023YFC3009300), the Alexander von Humboldt Foundation for the postdoctoral grant of Xuan-Yi Zhang, and the Henriette Herz Scouting program (Matthias G.R. Faes). The supports are gratefully acknowledged.

Appendix A. Procedure of classical reliability analysis methods combining with TIPP method

The proposed TIPP method can be integrated with classical reliability analysis techniques to determine the bounds of failure probability, where parametric p-boxes are replaced by general distributions associated with these bounds. The detailed procedures for applying TIPP method in combination with FORM, SORM, and the method of moments are discussed separately below.

A.1. FORM combining with TIPP method

In FORM, the reliability index is obtained by finding the shortest distance from the origin in the standard normal space to the linearization of the LSF. An iterative algorithm is used to determine the reliability index in classical FORM [22,23]. The iterative steps of FORM combining with TIPP method are summarized as follows:

(1) **Initialization:** Initialize the random variables in the standard normal space, denoted as $\mathbf{u}^{(k)}$ with $k = 0$. Typically, $\mathbf{u}^{(0)}$ is set as a vector with relatively small positive values.
(2) **Iteration:** Obtain a new iteration point as follows:

$$\mathbf{u}^{(k+1)} = \frac{1}{\nabla^T G_U(\mathbf{u}^{(k)}) \nabla G_U(\mathbf{u}^{(k)})} \left[\nabla^T G_U(\mathbf{u}^{(k)}) \mathbf{u}^{(k)} - G_U(\mathbf{u}^{(k)})\right] \nabla G_U(\mathbf{u}^{(k)}), \tag{A.1}$$

where $\nabla G_U(\mathbf{u}^{(k)})$ is the gradient of the performance function with respect to $\mathbf{u}^{(\mathbf{k})}$. The value of performance function and gradient vector at $\mathbf{u}^{(k)}$ can be calculated as follows:

$$G_U(\mathbf{u}^{(k)}) = G(\mathbf{x}^{(k)}), \tag{A.2}$$

$$\nabla G_U(\mathbf{u}^{(k)}) = \mathbf{J}^T \nabla G(\mathbf{x}^{(k)}), \tag{A.3}$$

where $\mathbf{J}$ is the Jacobian matrix. For independent $\mathbf{X}$, $\mathbf{J}$ can be expressed as:

$$\mathbf{J} = \frac{\partial \mathbf{x}^{(k)}}{\partial \mathbf{u}^{(k)}} = \begin{bmatrix} \frac{\partial \varphi(u_1)}{\partial f_{X_1}(x_1)} & 0 & \cdots & 0 \\ 0 & \frac{\partial \varphi(u_2)}{\partial f_{X_2}(x_2)} & \cdots & 0 \\ \vdots & \vdots & \ddots & \vdots \\ 0 & 0 & \cdots & \frac{\partial \varphi(u_n)}{\partial f_{X_n}(x_n)} \end{bmatrix}. \tag{A.4}$$

where $f_{X_i}(x_i)$ is the PDF of X_i. $\mathbf{x}^{(k)}$ is transformed from $\mathbf{u}^{(k)}$ using the inverse normal transformation, which is defined based on $\mathbf{\Theta}_{\text{low}}$ or $\mathbf{\Theta}_{\text{up}}$ for the lower and upper bounds of failure probability.
(3) **Convergence check:** Repeat steps (2) and (3) until convergence is achieved. The convergence criteria can be defined as follows:

$$\|\mathbf{u}^{(k+1)} - \mathbf{u}^{(k)}\| < \epsilon\,. \tag{A.5}$$

where ϵ is the allowable error.
(4) **Calculation of reliability index:** Calculate reliability index using the following formula:

$$\beta_F = \|\mathbf{u}^{(k+1)}\|\,. \tag{A.6}$$

A.2. SORM combining with TIPP method

SORM approximates the LSF using a quadratic Taylor series expansion, capturing nonlinear properties and thereby improving the accuracy of reliability analysis. The procedure for combining SORM with TIPP method is similar to that of FORM and is summarized as follows:

(1) **Initialization:** Initialize the random variables in the standard normal space, denoted as $\mathbf{u}^{(k)}$ with $k=0$. Typically, $\mathbf{u}^{(0)}$ is set as a vector with relatively small positive values.
(2) **Approximation of performance function:** Fit the performance function by the following second-order polynomial:

$$G_S(\mathbf{U}) = a_0 + \sum_{j=1}^{n} \gamma_j u_j + \sum_{j=1}^{n} \lambda_j u_j^2, \tag{A.7}$$

where a_0, γ_j and λ_j are regression coefficients, which are obtained using the point-fitting procedure with the fitting points selected around $\mathbf{u}^{(k)}$ [24]. Note that, in the point-fitting procedure, fitting points in standard normal space need to be transformed into original space with the aid of inverse normal transformation, where the moments applied are $\boldsymbol{\Theta}_{\text{low}}$ or $\boldsymbol{\Theta}_{\text{up}}$ for lower and upper bounds of failure probability, respectively.
(3) **Iteration**: Based on the approximated performance function $G_S(\mathbf{U})$ given in Eq. (A.7), perform FORM as discussed in Appendix A.1. The point corresponding to the first order reliability index is denoted as $\mathbf{u}^{(k+1)}$.
(4) **Convergence check:** If the convergence criteria given in Eq. (A.5) is achieved, go to next step, otherwise repeat steps (2) and (3) with $\mathbf{u}^{(k)}$ set to be $\mathbf{u}^{(k+1)}$.
(5) **Calculation of reliability index:** The second-order reliability index β_S can be obtained based on $\mathbf{u}^{(k+1)}$ as follows [35]:

$$\beta_S = \begin{cases} -\Phi^{-1}\left[\Phi(-\beta_F)\left(1+\dfrac{\phi(\beta_F)}{R\Phi(-\beta_F)}\right)^{-(n-1)/2[1+2K_s/10(1+2\beta_F)]}\right], & K_s \geq 0, \\ \left(1+\dfrac{2.5K_s}{2n-5R+25(23-5\beta_F)/R^2}\right)\beta_F + \dfrac{1}{2}K_s\left(1+\dfrac{K_s}{40}\right), & K_s < 0, \end{cases} \tag{A.8}$$

where

$$K_s = \frac{2}{|\nabla G_S(\mathbf{u}^{(k+1)})|}\sum_{j=1}^{n}\lambda_j\left[1-\frac{1}{|\nabla G_S(\mathbf{u}^{(k+1)})|^2}\left(\gamma_j+2\lambda_j u_j^{(k+1)}\right)^2\right], \tag{A.9}$$

$$R = \frac{n-1}{K_S}. \tag{A.10}$$

A.3. Method of moments combining with TIPP method

The method of moments treats the performance function $G(\mathbf{X})$ as a random variable Z, transforming the calculation of the failure probability from an integration over the JPDF of $\mathbf{X}$ to the CDF of Z at $Z=0$. In this paper, the distribution of Z is approximated using its first three moments, and the reliability index are computed as follows:

$$\beta_{3M} = -S^{-1}(0|\boldsymbol{\theta}_G), \tag{A.11}$$

where $S^{-1}(\cdot|\cdot)$ denotes the normal transformation, serving as the inverse function of $S(\cdot|\cdot)$ as defined in Eq. (13); $\boldsymbol{\theta}_G = \{\mu_G, \sigma_G, \alpha_{3G}\}$ is the first three moments of Z; and μ_G, σ_G and α_{3G} are the mean, standard deviation and skewness of $G(\mathbf{X})$, respectively.

One of the key tasks for the method of moments is to determine $\boldsymbol{\theta}_G$, which can be obtained from the first three original moments, denoted as μ_{kG} with $k=1,2,3$, as follows:

$$\mu_G = \mu_{1G}, \tag{A.12}$$

$$\sigma_G = \sqrt{\mu_{2G}-\mu_{1G}^2}, \tag{A.13}$$

$$\alpha_{3G} = (\mu_{3G}-3\mu_{2G}\mu_{1G}+2\mu_{1G}^3)/\sigma_G^3. \tag{A.14}$$

Due to the complexity of $G(\mathbf{X})$, there is generally no analytical solutions to μ_{kG}. To make a good balance between accuracy and efficiency, in this study, μ_{kG} is approximated using the five point-estimate method combined with bivariate dimension reduction method as follows [36,37]:

$$\mu_{kG} \approx \sum_{i<j}\mu_{k-i,j} - (n-2)\sum_i \mu_{k-i} + \frac{(n-1)(n-2)}{2}L_0^k, \tag{A.15}$$

$$\mu_{k-i,j} = \sum_{r_i=1}^{m}\sum_{r_j=1}^{m} P_{r_i}P_{r_j}\{G[\mu_1,\ldots,S(u_{r_i}|\theta_i),\ldots,S(u_{r_j}|\theta_j),\ldots,\mu_n]\}^k, \tag{A.16}$$

$$\mu_{k-i} = \sum_{r_i=1}^{m} P_{r_i}\{G[\mu_1,\ldots,S(u_{r_i}|\theta_i),\ldots,\mu_n]\}^k, \tag{A.17}$$

$$L_0^k = [G(\mu_1, \ldots, \mu_i, \ldots, \mu_n)]^k, \tag{A.18}$$

where u_{r_i} is the ith estimating point, and P_{r_i} is the corresponding weight. For five point estimate method, the estimate points $\mathbf{u_r}$ and corresponding weights $\mathbf{P_r}$ are given as follows:

$$\mathbf{u_r} = \{\pm 2.8570, \pm 1.3557, 0\}, \quad \mathbf{P_r} = \{0.0126, 0.2221, 0.5333\}. \tag{A.19}$$

The values of θ_i are used to compute the original moments of $Z = G(\mathbf{X})$, as given in Eqs. (A.16)–(A.18). With the aid of Table 1, these moments are taken as the values of $\mathbf{\Theta}_{\text{up}}$ and $\mathbf{\Theta}_{\text{low}}$ for upper and lower bounds of failure probability, respectively.

References

[1] E. Nikolaidis, D.M. Ghiocel, S. Singhal, Engineering Design Reliability Handbook, CRC press, 2004.
[2] M. Beer, S. Ferson, V. Kreinovich, Imprecise probabilities in engineering analyses, Mech. Syst. Signal Process. 37 (1) (2013) 4–29. https://doi.org/10.1016/j.ymssp.2013.01.024
[3] L.G. Crespo, S.P. Kenny, D.P. Giesy, Reliability analysis of polynomial systems subject to p-box uncertainties, Mech. Syst. Signal Process. 37 (1) (2013) 121–136. https://doi.org/10.1016/j.ymssp.2012.08.012
[4] M.G.R. Faes, M. Daub, S. Marelli, E. Patelli, M. Beer, Engineering analysis with probability boxes: a review on computational methods, Struct. Saf. 93 (2021) 102092. https://doi.org/10.1016/j.strusafe.2021.102092
[5] H. Zhang, R.L. Mullen, R.L. Muhanna, Interval Monte Carlo methods for structural reliability, Struct. Saf. 32 (3) (2010) 183–190. https://doi.org/10.1016/j.strusafe.2010.01.001
[6] H. Zhang, Interval importance sampling method for finite element-based structural reliability assessment under parameter uncertainties, Struct. Saf. 38 (2012) 1–10. https://doi.org/10.1016/j.strusafe.2012.01.003
[7] M.C.M. Troffaes, Imprecise Monte Carlo simulation and iterative importance sampling for the estimation of lower previsions, Int. J. Approx. Reason. 101 (2018) 31–48. https://doi.org/10.1016/j.ijar.2018.06.009
[8] M.G.R. Faes, M.A. Valdebenito, X. Yuan, P. Wei, M. Beer, Augmented reliability analysis for estimating imprecise first excursion probabilities in stochastic linear dynamics, Adv. Eng. Softw. 155 (2021) 102993. https://doi.org/10.1016/j.advengsoft.2021.102993
[9] X.K. Yuan, M.G.R. Faes, S.L. Liu, M.A. Valdebenito, M. Beer, Efficient imprecise reliability analysis using the augmented space integral, Reliab. Eng. Syst. Saf. 210 (2021) 107477. https://doi.org/10.1016/j.ress.2021.107477
[10] P.F. Wei, J.W. Song, S.F. Bi, M. Broggi, M. Beer, Z.Z. Lu, Z.F. Yue, Non-intrusive stochastic analysis with parameterized imprecise probability models: I. Performance estimation, Mech. Syst. Signal Process. 124 (2019) 349–368. https://doi.org/10.1016/j.ymssp.2019.01.058
[11] R.R.P. Callens, M. Faess, D. Moens, Multilevel Quasi-Monte Carlo for interval analysis, Int. J. Uncertain. Quantif. 12 (4) (2022) 1–19. https://doi.org/10.1615/Int.J.UncertaintyQuantification.2022039245
[12] Z.P. Qiu, D. Yang, I. Elishakoff, Combination of structural reliability and interval analysis, Acta Mech. Sin. 24 (1) (2008) 61–67. https://doi.org/10.1007/s10409-007-0111-4
[13] C. Jiang, W.X. Li, X. Han, L.X. Liu, P.H. Le, Structural reliability analysis based on random distributions with interval parameters, Comput. Struct. 89 (23-24) (2011) 2292–2302. https://doi.org/10.1016/j.compstruc.2011.08.006
[14] C. Jiang, X. Han, W.X. Li, J. Liu, Z. Zhang, A hybrid reliability approach based on probability and interval for uncertain structures, J. Mech. Des. 134 (3) (2012) 031001. https://doi.org/10.1115/1.4005595
[15] C. Wang, H. Zhang, M. Beer, Computing tight bounds of structural reliability under imprecise probabilistic information, Comput. Struct. 208 (2018) 92–104. https://doi.org/{10.1016/j.compstruc.2018.07.003}
[16] M.G.R. Faes, M.A. Valdebenito, D. Moens, M. Beer, Bounding the first excursion probability of linear structures subjected to imprecise stochastic loading, Comput. Struct. 239 (2020) 106320. https://doi.org/10.1016/j.compstruc.2020.106320
[17] M.G.R. Faes, M.A. Valdebenito, D. Moens, M. Beer, Operator norm theory as an efficient tool to propagate hybrid uncertainties and calculate imprecise probabilities, Mech. Syst. Signal Process. 152 (2021) 107482. https://doi.org/10.1016/j.ymssp.2020.107482
[18] B.Y. Wang, X.Y. Zhang, Y.G. Zhao, Third moment method for reliability analysis with uncertain moments characterized as interval variables, Struct. Saf. 111 (2024) 102499. https://doi.org/10.1016/j.strusafe.2024.102499
[19] Y.G. Zhao, T. Ono, Third-moment standardization for structural reliability analysis, J. Struct. Eng. 126 (2000) 724–732. https://doi.org/10.1061/(ASCE)0733-9445(2000)126:6(724)
[20] Y.G. Zhao, Z.H. Lu, T. Ono, A simple third-moment method for structural reliability, J. Asian Archit. Build. Eng. 5 (1) (2006) 129–136. https://doi.org/10.3130/jaabe.5.129
[21] Q. Qin, X.Y. Zhang, Z.H. Lu, Y.G. Zhao, Simplified third-order normal transformation and its application in structural reliability analysis, Eng. Mech. 37 (12) (2020) 78–86, 113. (in Chinese) https://doi.org/10.6052/j.issn.1000-4750.2020.01.0015
[22] A.M. Hasofer, N.C. Lind, Exact and invariant second-moment code format, J. Eng. Mech. Div. 100 (1) (1974) 111–121. https://doi.org/10.1061/JMCEA3.0001848
[23] R. Rackwitz, B. Fiessler, Structural reliability under combined random load sequences, Comput. Struct. 9 (5) (1978) 489–494. https://doi.org/10.1016/0045-7949(78)90046-9
[24] Y.G. Zhao, T. Ono, New approximations for SORM: part 2, J. Eng. Mech. 125 (1) (1999) 86–93. https://doi.org/10.1061/(ASCE)0733-9399(1999)125:1(86)
[25] K. Breitung, SORM, Design points, subset simulation, and Markov chain Monte Carlo, ASCE-ASME J. Risk Uncertain. Eng. Syst., Part A Civ. Eng. 7 (4) (2021) 04021052. https://doi.org/10.1061/AJRUA6.0001166
[26] Y.G. Zhao, Z.H. Lu, Structural Reliability: Approaches from Perspectives of Statistical Moments, Wiley, 2021. https://doi.org/10.1002/9781119620754
[27] C.H. Acevedo, X.Y. Zhang, M.A. Valdebenito, M.G.R. Faes, Reliability analysis combining method of moments with control variates, Probab. Eng. Mech. 81 (2025) 103771. https://doi.org/10.1016/j.probengmech.2025.103771
[28] Y.G. Zhao, T. Ono, M. Kato, Second-order third-moment reliability method, J. Struct. Eng. 128 (8) (2002) 1087–1090. https://doi.org/10.1061/(ASCE)0733-9445(2002)128:8(1087)
[29] J. Xu, T. Zhang, L. Li, Q.F. Yu, Structural reliability analysis with parametric p-box uncertainties via a Bayesian updating BDRM, Comput. Methods Appl. Mech. Eng. 432 (2024) 117377. https://doi.org/10.1016/j.cma.2024.117377
[30] J.E. Hurtado, Assessment of reliability intervals under input distributions with uncertain parameters, Probab. Eng. Mech. 32 (2013) 80–92. https://doi.org/10.1016/j.probengmech.2013.01.004
[31] Y.G. Zhao, X.Y. Zhang, Z.H. Lu, Complete monotonic expression of the fourth-moment normal transformation for structural reliability, Comput. Struct. 196 (2018) 186–199. https://doi.org/10.1016/j.compstruc.2017.11.006
[32] T. Igusa, A. Der Kiureghian, Dynamic characterization of two-degree-of-freedom equipment-structure systems, J. Eng. Mech. 111 (1) (1985) 1–19. https://doi.org/10.1061/(ASCE)0733-9399(1985)111:1(1)
[33] M.A. Valdebenito, H.A. Jensen, H.B. Hernández, L. Mehrez, Sensitivity estimation of failure probability applying line sampling, Reliab. Eng. Syst. Saf. 171 (2018) 99–111. https://doi.org/10.1016/j.ress.2017.11.010
[34] K.J. Bathe, Finite Element Procedures, Klaus-Jurgen Bathe, 2006.
[35] Y.G. Zhao, T. Ono, New approximations for SORM: part 1, J. Eng. Mech. 125 (1) (1999) 79–85. https://doi.org/10.1061/(ASCE)0733-9399(1999)125:1(79)

[36] Y.G. Zhao, T. Ono, New point estimates for probability moments, J. Eng. Mech. 126 (4) (2000) 433–436. https://doi.org/10.1061/(ASCE)0733-9399(2000)126:4(433)
[37] H. Xu, S. Rahman, A generalized dimension-reduction method for multidimensional integration in stochastic mechanics, Int. J. Numer. Methods Eng. 61 (12) (2004) 1992–2019. https://doi.org/10.1002/nme.1135